

Spin Hall magnetoresistance in Pt/(Ga,Mn)N devices

J. Aaron Mendoza-Rodarte^{1,2*}, Katarzyna Gas^{3,4}, Manuel Herrera-Zaldívar², Detlef Hommel⁵, Maciej Sawicki^{3,6}, and Marcos H. D. Guimarães^{1*}

¹*Zernike Institute for Advanced Materials, University of Groningen, 9747 AG Groningen, The Netherlands*

²*Centro de Nanociencias y Nanotecnología-Universidad Nacional Autónoma de México, Ensenada, 22800-Baja California, México*

³*Institute of Physics, Polish Academy of Sciences, Aleja Lotnikow 32/46, PL-02668 Warsaw, Poland*

⁴*Center for Science and Innovation in Spintronics, Tohoku University, Katahira 2-1-1, Aoba-ku, Sendai 980-8577, Japan*

⁵*Lukasiewicz Research Network - PORT Polish Center for Technology Development, Stabłowicka 147, Wrocław, Poland*

⁶*Research Institute of Electrical Communication, Tohoku University, Katahira 2-1-1, Aoba-ku, Sendai 980-8577, Japan*

E-mail: j.a.mendoza.rodarte@rug.nl, m.h.guimaraes@rug.nl

Diluted magnetic semiconductors (DMS) have attracted significant attention for their potential in spintronic applications. Particularly, magnetically-doped GaN is highly attractive due to its high relevance for the CMOS industry and the possibility of developing advanced spintronic devices which are fully compatible with the current industrial procedures. Despite this interest, there remains a need to investigate the spintronic parameters that characterize interfaces within these systems. Here, we perform spin Hall magnetoresistance (SMR) measurements to evaluate the spin transfer at a Pt/(Ga,Mn)N interface. We determine the transparency of the interface through the estimation of the real part of the spin mixing conductance finding $G_r = 2.6 \cdot 10^{14} \Omega^{-1} \text{ m}^{-2}$, comparable to state-of-the-art yttrium iron garnet (YIG)/Pt interfaces. Moreover, the magnetic ordering probed by SMR above the (Ga,Mn)N Curie temperature T_C provides a broader temperature range for the efficient generation and detection of spin currents, relaxing the conditions for this material to be applied in new spintronic devices.

Recent advances in the manipulation of electron charge and spin have highlighted spintronics as a key area of research^{1,2}. This interest stems from the potential of spintronic devices to address the limitations of traditional charged-based devices, such as high energy consumption³. Among various materials, diluted magnetic semiconductors (DMS), those systems where a fraction of cations are substituted by magnetic elements, stand out as promising candidates for spintronic applications due to their unique integration of semiconductor and magnetic properties⁴. Particularly, Mn-doped compounds have received significant attention from the research community since the formation of a ferromagnetic order at technologically relevant temperatures was predicted⁵ and successfully realized⁶. Among these compounds, single-phase Mn-doped GaN epitaxial layers stand out for their insulating and short-range ferromagnetic character at low temperatures. It presents a rich playground to explore magnetic interactions of magnetic ions in a semiconductor lattice. A brief discussion on the ferromagnetic mechanisms in (Ga,Mn)N is included in the supplementary material. The combination of these factors, coupled with GaN well-established roles in optoelectronics⁷, high-frequency^{8,9}, and power electronics¹⁰ could provide substantial technological benefits, particularly in the development of new GaN-based spintronic devices¹¹. In fact apart from exploitation of the magnetoelectric effect in (Ga,Mn)N so far¹², the study of GaN-based DMS has been focused on optimizing growth conditions¹³ and magnetic properties^{14,15}, while spin transport dynamics received comparatively less attention^{16–20}. It is therefore timely and important to exploit spintronic and magnonic²¹ properties of this insulating ferromagnetic material in an aim to foster the development of all-nitride low power information processing and dissipationless communication means based on spin waves propagation.

Of particular importance for new nonvolatile magnetic data storage applications, the field of spin-orbit torques (SOTs) focuses on manipulating the magnetization in thin film heterostructures via electric currents, providing a promising way to manipulate magnetization at the nanoscale²². This technology relies on transferring spin angular momentum from a normal metal into a ferromagnet, using spin-charge interconversion effects to exert a torque on the magnetization²². Significant advancements in SOT have catalyzed the development of non-volatile memory devices^{23,24}. However, the success of these devices depends on efficient generation, transport, and detection of spin currents. While material research with high spin-orbit coupling²⁵ or orbital angular momentum effects²⁶ addresses spin current generation,

transport issues are managed by identifying materials with high interface spin transparency, indicated by substantial spin mixing conductance values ($G_{\uparrow\downarrow}$). Spin Hall magnetoresistance (SMR) has emerged as a key technique for assessing spin transport properties at heterostructure interfaces through electrical methods²⁷. Despite these advances, there is still a significant gap in understanding spin transport properties in heterostructures that utilize transition metal-doped GaN, which is crucial for SOT applications.

In this study, we investigate spin Hall magnetoresistance (SMR) within a Pt/(Ga,Mn)N heterostructure. By performing angle-dependent magnetoresistance measurements, we determine the spin mixing conductance ($G_{\uparrow\downarrow}$), a critical parameter that dictates the transport of spin information through the interface between the two materials. Additionally, we provide another assessment of the Curie temperature of the magnetic layer solely through electrical means, via temperature-dependent measurements. Our results provide valuable insights for the development of devices that incorporate GaN-based DMS for advanced spintronic applications.

To characterize the Pt/(Ga,Mn)N interface via SMR, we fabricated a 6 nm-thick Pt Hall bar on a 100 nm-thick single-phase epitaxy $\text{Ga}_{0.922}\text{Mn}_{0.078}\text{N}$ film. The film was grown using plasma-assisted molecular beam epitaxy (MBE) on a 3 μm -thick GaN(0001) template, which was deposited on *c*-oriented 2-inch sapphire substrates. Detailed methodologies for the growth and magnetic and crystallographic characterization of these films are discussed in detail in reference¹⁴. The Hall bar, measuring 25 μm in wide and 200 μm in length, was fabricated by conventional lithography processes. Prior to the deposition of Pt through Ar^+ plasma d.c. sputtering, the (Ga,Mn)N surface was cleaned using an Ar^+ mild etching process, detailed in supplementary material. Electrical measurements were performed by rotating an external magnetic field within the plane of the device. We utilized conventional lock-in techniques for the measurements, with a bias current (I_{bias}) of less than 0.7 mA at a frequency of 187.77 Hz. This setup allowed us to measure the transverse resistance (R_{xy}), which is perpendicular to the current path. This layout of the electrical interconnects is illustrated in Fig. 1(a).

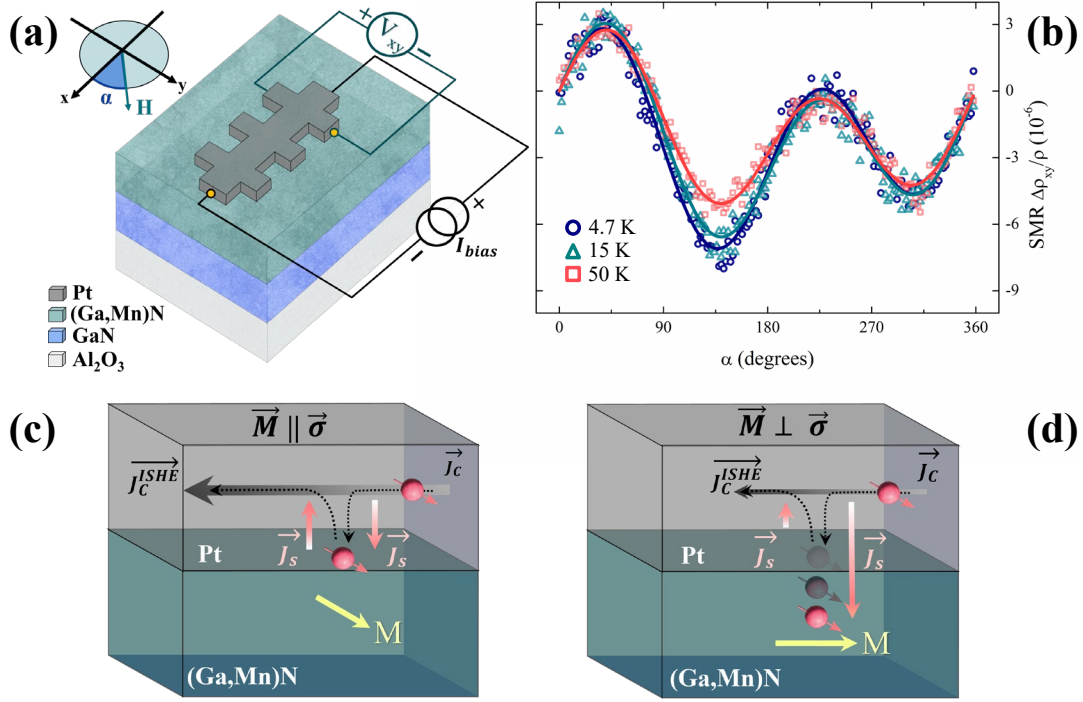


FIG. 1. (a) Schematics of the devices and electrical measurement configuration, illustrating the definition of the rotating external magnetic field angle α . (b) Angle dependence of the SMR signal in the transverse geometry as a function of α . The measurements were conducted in the temperature range of 4.7 to 50 K using an external magnetic field of 600 mT. A baseline has been removed so that the relative changes in resistivity are zero at $\alpha=0$ degrees. (c-d) Schematic representation of SMR. (c) Low-resistance configuration where $\vec{M} \parallel \vec{\sigma}$. (d) High-resistance configuration where $\vec{M} \perp \vec{\sigma}$.

The SMR measurements offer insights into the magnetic ordering at the surface of the (Ga,Mn)N thin film at low temperatures. Fig. 1(b) illustrates the dependence of the magnetic field angle (α) on the relative changes in the transverse resistivity, $\Delta\rho_{xy}/\rho$. Here, $\Delta\rho_{xy}/\rho$ is defined as $(R_{xy} - R_{0,xy})/(R_{0,xx}/4.8)$ where R_{xy} is the transverse resistance, and $R_{0,xy}$ and $R_{0,xx}$ are the transverse and longitudinal resistances at zero magnetic field, respectively, and 4.8 is the geometrical factor of the Hall bar (length/width). The observed changes in resistivity can be explained as follows: when a charge current (J_c) flows through Pt, the spin Hall effect (SHE) induces a transverse spin current (J_s) towards the (Ga,Mn)N/Pt interface. At this interface, spin accumulation interacts with the local magnetic moments of (Ga,Mn)N. If the spin polarization $\vec{\sigma}$ is parallel to the magnetization direction \vec{M} of the ferromagnet ($\vec{M} \parallel \vec{\sigma}$), the electrons' angular momentum is reflected, resulting in a low-resistance configuration due to the inverse spin Hall effect (ISHE) [see Fig. 1(c)]. Conversely, when \vec{M} is perpendicular to $\vec{\sigma}$ ($\vec{M} \perp \vec{\sigma}$) [refer to Fig. 1(d)], the electrons' angular momentum is absorbed, leading to a high-resistance configuration. In transverse SMR measurements, the interaction of the generated

spin current with the (Ga,Mn)N magnetization \vec{M} at the interface results in a reorientation of the outgoing spin current polarization $\vec{\sigma}$. At angles $\alpha = 45^\circ$ and 135° , this leads to positive and negative transverse voltage, respectively²⁸. Our experimental observations align with this theory, showing maximum resistance at $\alpha = 45^\circ$ and minimum at $\alpha = 135^\circ$, similar to findings in YIG/Pt systems²⁹. The dependence of the resistivity in the transverse geometry (ρ_T) with respect to the magnetization components along the different directions is given by²⁷:

$$\rho_T = \Delta\rho_1 m_x m_y + \Delta\rho_2 m_z + \Delta\rho_{Hall} B_z, \quad (1)$$

where $\Delta\rho_1$ and $\Delta\rho_2$ represents relative changes in resistivity and m_x , m_y , and m_z are the components (unit vectors) of magnetization in the \hat{x} -, \hat{y} - and \hat{z} -direction, respectively. The angular dependencies are defined by the components m_x , m_y , and m_z , where $m_x = \cos(\alpha) \cos(\beta)$, $m_y = \sin(\alpha) \cos(\beta)$, and $m_z = \sin(\beta)$, with β representing the azimuthal angle – i.e. the angle with respect to the out-of-plane (OOP) direction. Using these definitions, we can express the change in the transverse resistivity as follows²⁷:

$$\Delta\rho_{xy}/\rho = \Delta\rho_{xy,1} \frac{1}{2} \sin(2\alpha) - \Delta\rho_{xy,2} \sin(\beta), \quad (2)$$

where $\Delta\rho_{xy,1}$ and $\Delta\rho_{xy,2}$ represent the amplitudes of the relative change in resistivity.²⁶ This equation effectively describes our observed signals and fits our measurements well. Additionally, the term $\Delta\rho_{Hall} B_z$ accounts for the ordinary Hall effect occurring in Pt when a magnetic field is applied in the \hat{z} -direction. The $\sin(\beta)$ component observed in our results likely results from OOP component due to misalignment of the Hall bar with respect to the in-plane field. At 4.7 K, the values for the amplitudes $\Delta\rho_{xy,1}$ and $\Delta\rho_{xy,2}$ are $7.2 \cdot 10^{-6}$ and $1.8 \cdot 10^{-6}$, respectively, indicating a clear dominance of the in-plane component.

Using SMR measurements, we investigate the ferromagnetic-paramagnetic transition of (Ga,Mn)N solely through electrical methods. To this end, we perform a temperature-dependent measurement ranging from 4.7 to 290 K. Fig. 2 displays the behavior of magnitudes $\Delta\rho_{xy,1}$ and $\Delta\rho_{xy,2}$ derived from Eq. (1) across different temperatures. As the temperature increased from 4.7 to 10 K, $\Delta\rho_{xy,1}$ fluctuated between $7.2 \cdot 10^{-6}$ and $7.3 \cdot 10^{-6}$ with the maximum value at 10 K. Above 10 K, a decrease in $\Delta\rho_{xy,1}$ was noted, dropping to $6.81 \cdot 10^{-6}$ at 15 K. This reduction in the SMR signal suggests a T_C between 10 to 15 K, aligning well with the T_C of 13.0 ± 0.3 K established by SQUID magnetometry¹⁴. The signal diminished above 50 K, and data fitting became unreliable due to a significant decrease in the signal-to-noise ratio (SNR).

Nevertheless, it is important to note that substantial SMR signals have been observed from 15 to 50 K, a range dominated by the paramagnetic phase. This magnetic ordering is similar to that seen in other Curie-like paramagnetic insulators such as $\text{Gd}_3\text{Ga}_5\text{O}_{12}$ (GGG)^{30,31}. In such materials, the SMR arises from the interaction between the conduction-electron spins in Pt and the paramagnetic spins S within GGG via the interface exchange interaction, which applies torque on S . Regarding the fitted OOP component, its temperature dependence displayed a monotonic behavior, with $\Delta\rho_{xy,2}$ values between 1.6 and $1.9 \cdot 10^{-6}$. This points towards an ordinary Hall contribution in our transverse measurements, which can be attributed to a sample misalignment.

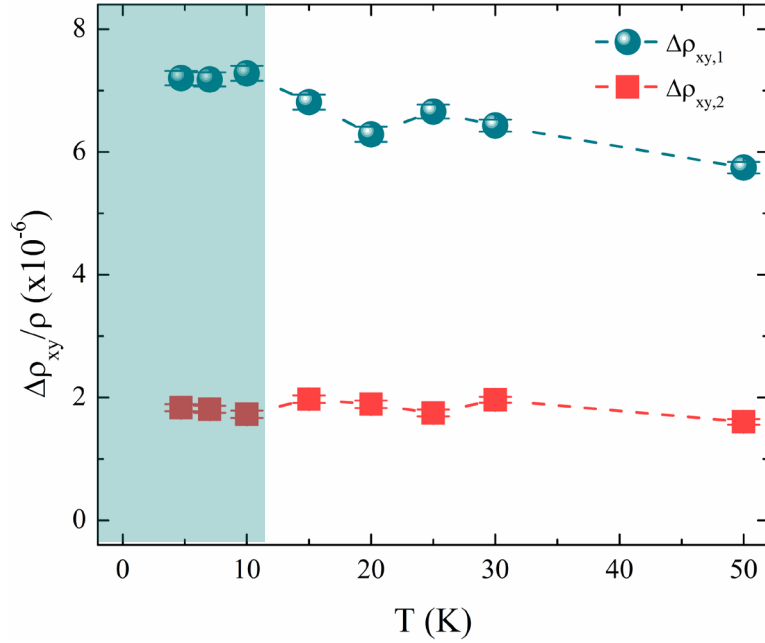


FIG. 2. Temperature dependence of the relative changes of the resistivity of $\Delta\rho_{xy,1}$ and $\Delta\rho_{xy,2}$. The green shadow highlights the decrease of the SMR signal observed above 10 K. All the amplitudes were extracted from Eq. (1) using measurements performed at 600 mT.

The magnetic field dependence of $\Delta\rho_{xy,1}$ and $\Delta\rho_{xy,2}$ demonstrates quadratic and linear behaviors, respectively, as shown in Fig. 3a and 3b. We can attribute the former dependency to the percolating character of ferromagnetism in our material, indicating that only at $T=0$ all the spins present in the sample are ferromagnetically coupled. On increasing T some of the spins start decoupling such that at its equilibrium T_c only about 20% of spins remain in the infinite cluster³². The remaining spins reside in *finite* ferromagnetic clusters of different sizes. These magnetic granules are characterized by their own magnetic moments and are responsible for the glassy characteristics like blocking (i.e. as in the material being far from thermal

equilibrium). Such material can therefore mimic a ferromagnet well above its equilibrium T_c when it is probed on sufficiently short time scales, as during SMR experiments. Additionally, at 600 mT we do not observe a saturation state, a finding corroborated by SQUID magnetometry M - H curves, which indicate that even at $\mu_0 H = 7$ T at $T = 2$ K the system still exhibits a positive slope (as indicated in the supplementary material Fig. S2). The coercive field (H_c) values from SQUID magnetometry for similar samples suggest an increase of the average magnetization above 200 mT, aligning with the clear SMR signal observed at 240 mT in our results (Fig. 3a). Additionally, the linear dependence seen in $\Delta\rho_{xy,2}$ aligns with the expected behavior of the ordinary Hall component. To confirm that our measurements are within the linear regime, we conducted bias current (I_{bias}) dependence tests. Fig. 3c shows the transverse voltage (V_{xy}) as a function of α , and Fig. 3d displays the I_{bias} dependency of the relative change in transverse voltage ΔV_{xy} , where a data point represents the amplitude of the angle-dependent voltage, obtained by a fit to $V_{xy} = \Delta V_{xy,1} \frac{1}{2} \sin(2\alpha) - \Delta V_{xy,2} \sin(\beta)$. Linear fits applied to both the in-plane ($\Delta V_{xy,1}$) and out-of-plane ($\Delta V_{xy,2}$) components confirm the linear behavior, with no evident heating effects.

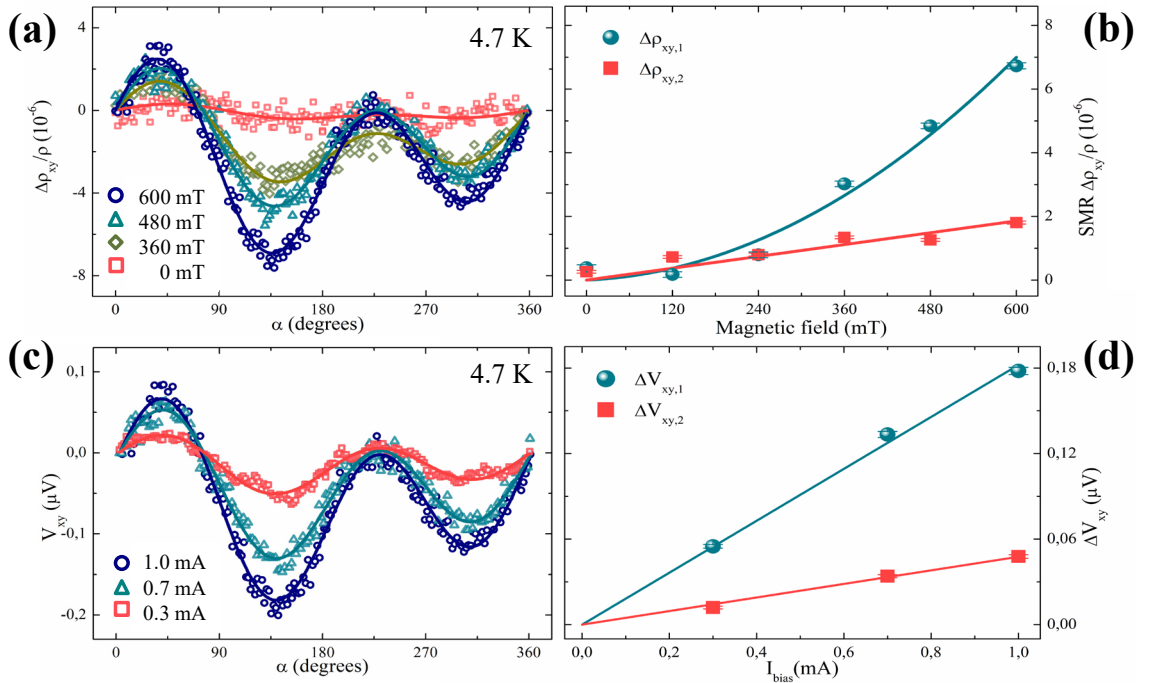


FIG. 3. (a) Relative change of the transverse resistivity ρ_{xy} as a function of angle α at different values of magnetic field B and for bias current $I_{bias}=1.0$ mA. (b) Magnetic field dependence of $\Delta\rho_{xy,1}$ and $\Delta\rho_{xy,2}$. (c) Angle dependence of V_{xy} at different I_{bias} . (d) Current dependence of ΔV_{xy} . All the measurements were performed at a fixed temperature of 4.7 K. A baseline has been removed so that the relative changes in resistivity are zero at $\alpha=0$ degrees.

The transfer of spin angular momentum at the interface of the heterostructure is quantified by the spin mixing conductance, $G_{\uparrow\downarrow}$, which we estimate from our experimental results. From Eq. (1), we can express $\Delta\rho_1$ and $\Delta\rho_2$ as follows²⁷:

$$\frac{\Delta\rho_1}{\rho} = \theta_{SH}^2 \frac{\lambda}{d_N} \operatorname{Re} \left(\frac{2\lambda G_{\uparrow\downarrow} \tanh^2 \frac{d_N}{\lambda}}{\sigma + 2\lambda G_{\uparrow\downarrow} \coth \frac{d_N}{\lambda}} \right), \quad (3)$$

$$\frac{\Delta\rho_2}{\rho} = -\theta_{SH}^2 \frac{\lambda}{d_N} \operatorname{Im} \left(\frac{2\lambda G_{\uparrow\downarrow} \tanh^2 \frac{d_N}{\lambda}}{\sigma + 2\lambda G_{\uparrow\downarrow} \coth \frac{d_N}{\lambda}} \right). \quad (4)$$

Here, θ_{SH} represents the spin Hall angle, λ the spin relaxation length, d_N the thickness, and σ the conductivity of Pt. $G_{\uparrow\downarrow}$ denotes the relaxation of the spin current polarization component transverse to the magnetization at the Pt/(Ga,Mn)N interface³³ and is defined as the sum of its real and imaginary parts ($G_{\uparrow\downarrow} = G_r + iG_i$). In our calculations the imaginary part is neglected due to its significantly smaller contribution compared to the real part³⁴.

The Pt conductivity $\sigma = 1/\rho$ is calculated from the resistivity measured by a four-probe method on the Pt Hall bar, yielding a value of $6.3 \cdot 10^6 \Omega^{-1} \text{ m}^{-1}$, consistent with literature values^{35–37}. Assuming constant values of $\theta_{SH} = 0.08$, $\lambda = 1.1 \pm 0.3 \text{ nm}$ ^{38,39}, taking $d_N = 6 \text{ nm}$, and using our SMR data at 4.7 K and $B = 600 \text{ mT}$, we calculate the real part of the spin mixing conductance, which under $G_{\uparrow\downarrow} \approx G_r$ condition attains a value of $2.6 \cdot 10^{14} \Omega^{-1} \text{ m}^{-2}$. This value is comparable to those reported for other heavy metal/magnetic insulator interfaces such as YIG/Pt³⁸.

Our study shows that the Pt/(Ga,Mn)N interface exhibits spintronic properties comparable to state-of-the-art systems, such as YIG/Pt interfaces³⁹, as evidenced by similar spin mixing conductance values. This indicates the strong potential of magnetically-doped GaN for spintronic and magnonic applications such as magnonic transistors⁴⁰ and SOT devices⁴¹. Furthermore, the magnetic ordering probed by SMR in (Ga,Mn)N above its equilibrium Curie temperature extends sizably the temperature range for efficient generating and detecting spin currents in this material. This broadens the operational parameters for its application in novel spintronic devices with higher operating temperatures. Our findings contribute significantly to understanding spin transport in (Ga,Mn)N-based devices and set the stage for exploring various device architectures for new spintronic applications based on the nitride family.

SUPPLEMENTARY MATERIAL

See [supplementary material \[url\]](#) for a brief discussion of the ferromagnetic mechanism in (Ga,Mn)N insulating systems, a detailed description of Pt/(Ga,Mn)N device fabrication, and SQUID magnetometry measurements, which includes Ref.^{12,14,32,42–60}.

ACKNOWLEDGMENTS

We acknowledge M. Cosset-Chéneau and J. J. L. van Rijn for helpful discussions and critically reading the manuscript, and J. Holstein, H. de Vries, F.H. van der Velde, H. Adema, and A. Joshua for technical support. This work was supported by the Dutch Research Council (NWO – OCENW.XL21.XL21.058), the Zernike Institute for Advanced Materials, the research program “Materials for the Quantum Age” (QuMat, registration number 024.005.006), which is part of the Gravitation program financed by the Dutch Ministry of Education, Culture and Science (OCW), the National Science Centre (Poland) through project OPUS (DEC-2018/31/B/ST3/03438), and the European Union (ERC, 2D-OPTOSPIN, 101076932, and 2DMAGSPIN, 101053054). Views and opinions expressed are however those of the author(s) only and do not necessarily reflect those of the European Union or the European Research Council. Neither the European Union nor the granting authority can be held responsible for them. JAMR is grateful to CONAHCYT for a graduate research fellowship (no. CVU 655591). The device fabrication and characterization were performed using Zernike NanoLabNL facilities.

AUTHOR DECLARATIONS

Conflict of Interest

The authors have no conflicts to disclose.

Author Contributions

J. Aaron Mendoza-Rodarte: Conceptualization (equal); Methodology (lead); Validation (lead); Formal analysis (lead); Investigation (lead); Data Curation (lead); Writing – Original Draft (lead); Visualization (equal). **Katarzyna Gas:** Resources (supporting); Writing – Review & Editing (supporting). **Manuel Herrera-Zaldívar:** Supervision (supporting); Writing – Review & Editing (supporting). **Detlef Hommel:** Resources (supporting); Writing – Review & Editing (supporting). **Maciej Sawicki:** Resources (supporting); Writing – Review & Editing

(supporting). **Marcos H. D. Guimarães:** Supervision (lead); Project administration (lead); Conceptualization (equal); Visualization (equal); Resources (lead); Writing – Review & Editing (lead); Funding acquisition (lead).

DATA AVAILABILITY

The data that support the findings of this study are available from the corresponding author upon reasonable request.

REFERENCES

- ¹ C. Song, R. Zhang, L. Liao, Y. Zhou, X. Zhou, R. Chen, Y. You, X. Chen, and F. Pan, “Spin-orbit torques: Materials, mechanisms, performances, and potential applications,” *Prog Mater Sci* **118**, 100761 (2021).
- ² B. Dieny, I.L. Prejbeanu, K. Garello, P. Gambardella, P. Freitas, R. Lehndorff, W. Raberg, U. Ebels, S.O. Demokritov, J. Akerman, A. Deac, P. Pirro, C. Adelman, A. Anane, A. V. Chumak, A. Hirohata, S. Mangin, S.O. Valenzuela, M.C. Onbaşlı, M. d’Aquino, G. Prenat, G. Finocchio, L. Lopez-Diaz, R. Chantrell, O. Chubykalo-Fesenko, and P. Bortolotti, “Opportunities and challenges for spintronics in the microelectronics industry,” *Nat Electron* **3**, 446–459 (2020).
- ³ S.A. Wolf, D.D. Awschalom, R.A. Buhrman, J.M. Daughton, S. Von Molnár, M.L. Roukes, A.Y. Chtchelkanova, and D.M. Treger, *Spintronics: A Spin-Based Electronics Vision for the Future Science* **294**, 1488–1495 (2001).
- ⁴ J.K. Furdyna, “Diluted magnetic semiconductors: An interface of semiconductor physics and magnetism (invited),” *J Appl Phys* **53**, 7637–7643 (1982).
- ⁵ T. Dietl, H. Ohno, F. Matsukura, J. Cibert, and D. Ferrand, “Zener Model Description of Ferromagnetism in Zinc-Blende Magnetic Semiconductors,” *Science* **287**, 1019–1022 (2000).
- ⁶ T. Dietl, and H. Ohno, “Dilute ferromagnetic semiconductors: Physics and spintronic structures,” *Rev Mod Phys* **86**, 187–251 (2014).
- ⁷ H.D. Jabbar, M.A. Fakhri, and M. Jalal AbdulRazzaq, “Gallium Nitride –Based Photodiode: A review,” *Mater Today Proc* **42**, 2829–2834 (2021).
- ⁸ W. Zhang, F. Wang, D.J. Costinett, L.M. Tolbert, and B.J. Blalock, “Investigation of Gallium Nitride Devices in High-Frequency LLC Resonant Converters,” *IEEE Trans Power Electron* **32**, 571–583 (2017).
- ⁹ M.T. Hibberd, V. Frey, B.F. Spencer, P.W. Mitchell, P. Dawson, M.J. Kappers, R.A. Oliver, C.J. Humphreys, and D.M. Graham, “Dielectric response of wurtzite gallium nitride in the terahertz frequency range,” *Solid State Commun* **247**, 68–71 (2016).
- ¹⁰ A. Udabe, I. Baraia-Etxaburu, and D.G. Diez, “Gallium Nitride Power Devices: A State of the Art Review,” *IEEE Access* **11**, 48628–48650 (2023).
- ¹¹ T.H. Dang, J. Hawecker, E. Rongione, G. Baez Flores, D.Q. To, J.C. Rojas-Sanchez, H. Nong, J. Mangeney, J. Tignon, F. Godel, S. Collin, P. Seneor, M. Bibes, A. Fert, M. Anane, J.M. George, L. Vila, M. Cosset-Cheneau, D. Dolfi, R. Lebrun, P. Bortolotti, K. Belashchenko, S. Dhillon, and H. Jaffrès, “Ultrafast spin-currents and charge conversion at 3 d-5 d interfaces probed by time-domain terahertz spectroscopy,” *Appl Phys Rev* **7**, 041409 (2020).
- ¹² D. Sztienkiel, M. Foltyn, G.P. Mazur, R. Adhikari, K. Kosiol, K. Gas, M. Zgierski, R. Kruska, R. Jakiela, T. Li, A. Piotrowska, A. Bonanni, M. Sawicki, and T. Dietl, “Stretching magnetism with an electric field in a nitride semiconductor,” *Nat Commun* **7**, 13232 (2016).
- ¹³ E. Piskorska-Hommel, and K. Gas, “(Ga,Mn)N—Epitaxial growth, structural, and magnetic characterization—Tutorial,” *J Appl Phys* **135**, 071101 (2024).

- ¹⁴ K. Gas, J.Z. Domagala, R. Jakiela, G. Kunert, P. Dłuzewski, E. Piskorska-Hommel, W. Paszkowicz, D. Sztenkiel, M.J. Winiarski, D. Kowalska, R. Szukiewicz, T. Baraniecki, A. Mischczuk, D. Hommel, and M. Sawicki, "Impact of substrate temperature on magnetic properties of plasma-assisted molecular beam epitaxy grown (Ga,Mn)N," *J Alloys Compd* **747**, 946–959 (2018).
- ¹⁵ K. Gas, D. Hommel, and M. Sawicki, "Raman scattering studies of the lateral Mn distribution in MBE-grown Ga_{1-x}Mn_xN epilayers," *J Alloys Compd* **817**, 152789 (2020).
- ¹⁶ R. Jakiela, K. Gas, M. Sawicki, and A. Barcz, "Diffusion of Mn in gallium nitride: Experiment and modelling," *J Alloys Compd* **771**, 215–220 (2019).
- ¹⁷ M. Aoki, H. Yamane, M. Shimada, and T. Kajiwara, "Single crystal growth of manganese gallium nitride using Mn-Ga-Na melt," *J Alloys Compd* **364**, 280–282 (2004).
- ¹⁸ Y. Ma, A. V. Chinchore, A.R. Smith, M.A. Barral, and V. Ferrari, "A Two-Dimensional Manganese Gallium Nitride Surface Structure Showing Ferromagnetism at Room Temperature," *Nano Lett* **18**, 158–166 (2018).
- ¹⁹ D. Tanaka, K. Iso, and J. Suda, "Comparative study of electrical properties of semi-insulating GaN substrates grown by hydride vapor phase epitaxy and doped with Fe, C, or Mn," *J Appl Phys* **133**, 055701 (2023).
- ²⁰ J.A. Carlson, M. Ganjoo, and J.M. Dallesasse, "Optical Transitions and Magnetism in Mn-Implanted Gallium Nitride for Three-Level Magneto-optic Devices," *IEEE Trans Electron Devices* **69**, 225–230 (2022).
- ²¹ A. V. Chumak, V.I. Vasyuchka, A.A. Serga, and B. Hillebrands, "Magnon spintronics," *Nat Phys* **11**, 453–461 (2015).
- ²² F. Binda, S. Fedel, S.F. Alvarado, P. Noël, and P. Gambardella, "Spin–Orbit Torques and Spin Hall Magnetoresistance Generated by Twin-Free and Amorphous Bi_{0.9}Sb_{0.1} Topological Insulator Films," *Advanced Materials* **35**, 2304905 (2023).
- ²³ H. Yang, S.O. Valenzuela, M. Chshiev, S. Couet, B. Dieny, B. Dlubak, A. Fert, K. Garello, M. Jamet, D.E. Jeong, K. Lee, T. Lee, M.B. Martin, G.S. Kar, P. S  n  or, H.J. Shin, and S. Roche, "Two-dimensional materials prospects for non-volatile spintronic memories," *Nature* **606**, 663–673 (2022).
- ²⁴ V. Krizakova, M. Perumkunnil, S. Couet, P. Gambardella, and K. Garello, "Spin-orbit torque switching of magnetic tunnel junctions for memory applications," *J Magn Magn Mater* **562**, 169692 (2022).
- ²⁵ O.L.W. McHugh, M. Gradhand, and D.A. Stewart, "Optimizing the spin Hall effect in Pt-based binary alloys," *Phys Rev Mater* **8**, 15003 (2024).
- ²⁶ D. Go, D. Jo, H.-W. Lee, M. Kl  ui, and Y. Mokrousov, "Orbitronics: Orbital currents in solids," *Europhys Lett* **135**, 37001 (2021).
- ²⁷ Y.T. Chen, S. Takahashi, H. Nakayama, M. Althammer, S.T.B. Goennenwein, E. Saitoh, and G.E.W. Bauer, "Theory of spin Hall magnetoresistance," *Phys Rev B* **87**, 144411 (2013).
- ²⁸ H. Nakayama, M. Althammer, Y.T. Chen, K. Uchida, Y. Kajiwara, D. Kikuchi, T. Ohtani, S. Gepr  gs, M. Opel, S. Takahashi, R. Gross, G.E.W. Bauer, S.T.B. Goennenwein, and E. Saitoh, "Spin Hall Magnetoresistance Induced by a Nonequilibrium Proximity Effect," *Phys Rev Lett* **110**, 206601 (2013).
- ²⁹ N. Vlietstra, J. Shan, V. Castel, B.J. Van Wees, and J. Ben Youssef, "Spin-Hall magnetoresistance in platinum on yttrium iron garnet: Dependence on platinum thickness and in-plane/out-of-plane magnetization," *Phys Rev B* **87**, 184421 (2013).
- ³⁰ K. Oyanagi, S. Takahashi, L.J. Cornelissen, J. Shan, S. Daimon, T. Kikkawa, G.E.W. Bauer, B.J. van Wees, and E. Saitoh, "Spin transport in insulators without exchange stiffness," *Nat Commun* **10**, 4740 (2019).
- ³¹ K. Oyanagi, J.M. Gomez-Perez, X.P. Zhang, T. Kikkawa, Y. Chen, E. Sagasta, A. Chuvilin, L.E. Hueso, V.N. Golovach, F.S. Bergeret, F. Casanova, and E. Saitoh, "Paramagnetic spin Hall magnetoresistance," *Phys Rev B* **104**, 134428 (2021).
- ³² I.Ya. Korenblit, E.F. Shender, and B.I. Shklovsky, "Percolation approach to the phase

transition in very dilute ferromagnetic alloys,” *Phys Lett A* **46**, 275–276 (1973).

³³ M. Cosset-Chéneau, L. Vila, G. Zahnd, D. Gusakova, V.T. Pham, C. Grèzes, X. Waintal, A. Marty, H. Jaffrès, and J.P. Attané, “Measurement of the Spin Absorption Anisotropy in Lateral Spin Valves,” *Phys Rev Lett* **126**, 027201 (2021).

³⁴ K. Xia, P.J. Kelly, G.E.W. Bauer, A. Brataas, and I. Turek, “Spin torques in ferromagnetic/normal-metal structures,” *Phys Rev B* **65**, 2204011 (2002).

³⁵ M.B. Jungfleisch, A. V. Chumak, V.I. Vasyuchka, A.A. Serga, B. Obry, H. Schultheiss, P.A. Beck, A.D. Karenowska, E. Saitoh, and B. Hillebrands, “Temporal evolution of inverse spin Hall effect voltage in a magnetic insulator-nonmagnetic metal structure,” *Appl Phys Lett* **99**, 182512 (2011).

³⁶ V. Castel, N. Vlietstra, J. Ben Youssef, and B.J. Van Wees, “Platinum thickness dependence of the inverse spin-Hall voltage from spin pumping in a hybrid yttrium iron garnet/platinum system,” *Appl Phys Lett* **101**, 132414 (2012).

³⁷ L. Baldtrati, A. Ross, T. Niizeki, C. Schneider, R. Ramos, J. Cramer, O. Gomonay, M. Filianina, T. Savchenko, D. Heinze, A. Kleibert, E. Saitoh, J. Sinova, and M. Kläui, “Full angular dependence of the spin Hall and ordinary magnetoresistance in epitaxial antiferromagnetic NiO(001)/Pt thin films,” *Phys Rev B* **98**, 024422 (2018).

³⁸ N. Vlietstra, J. Shan, V. Castel, J. Ben Youssef, G.E.W. Bauer, and B.J. Van Wees, “Exchange magnetic field torques in YIG/Pt bilayers observed by the spin-Hall magnetoresistance,” *Appl Phys Lett* **103**, 032401 (2013).

³⁹ G.R. Hoozeboom, A. Aqeel, T. Kuschel, T.T.M. Palstra, and B.J. Van Wees, “Negative spin Hall magnetoresistance of Pt on the bulk easy-plane antiferromagnet NiO,” *Appl Phys Lett* **111**, 052409 (2017).

⁴⁰ L.J. Cornelissen, J. Liu, B.J. van Wees, and R.A. Duine, “Spin-Current-Controlled Modulation of the Magnon Spin Conductance in a Three-Terminal Magnon Transistor,” *Phys Rev Lett* **120**, 97702 (2018).

⁴¹ A. Manchon, J. Železný, I.M. Miron, T. Jungwirth, J. Sinova, A. Thiaville, K. Garello, and P. Gambardella, “Current-induced spin-orbit torques in ferromagnetic and antiferromagnetic systems,” *Rev Mod Phys* **91**, 035004 (2019).

⁴² T. Dietl, F. Matsukura, and H. Ohno, “Ferromagnetism of magnetic semiconductors: Zhang-Rice limit,” *Phys Rev B* **66**, 33203 (2002).

⁴³ A. Bonanni, M. Sawicki, T. Devillers, W. Stefanowicz, B. Faina, T. Li, T.E. Winkler, D. Sztienkiel, A. Navarro-Quezada, M. Rovezzi, R. Jakiela, A. Grois, M. Wegscheider, W. Jantsch, J. Suffczyński, F. D’Acapito, A. Meingast, G. Kothleitner, and T. Dietl, “Experimental probing of exchange interactions between localized spins in the dilute magnetic insulator (Ga,Mn)N,” *Phys Rev B* **84**, 35206 (2011).

⁴⁴ T. Yamamoto, H. Sazawa, N. Nishikawa, M. Kiuchi, T. Ide, M. Shimizu, T. Inoue, and M. Hata, “Reduction in Buffer Leakage Current with Mn-Doped GaN Buffer Layer Grown by Metal Organic Chemical Vapor Deposition,” *Jpn J Appl Phys* **52**, 08JN12 (2013).

⁴⁵ R. Adhikari, W. Stefanowicz, B. Faina, G. Capuzzo, M. Sawicki, T. Dietl, and A. Bonanni, “Upper bound for the s - d exchange integral in n -(Ga,Mn)N:Si from magnetotransport studies,” *Phys Rev B* **91**, 205204 (2015).

⁴⁶ L. Janicki, G. Kunert, M. Sawicki, E. Piskorska-Hommel, K. Gas, R. Jakiela, D. Hommel, and R. Kudrawiec, “Fermi level and bands offsets determination in insulating (Ga,Mn)N/GaN structures,” *Sci Rep* **7**, 41877 (2017).

⁴⁷ K. Kalbarczyk, K. Dybko, K. Gas, D. Sztienkiel, M. Foltyn, M. Majewicz, P. Nowicki, E. Łusakowska, D. Hommel, and M. Sawicki, “Electrical characteristics of vertical-geometry Schottky junction to magnetic insulator (Ga,Mn)N heteroepitaxially grown on sapphire,” *J Alloys Compd* **804**, 415–420 (2019).

⁴⁸ J. Kreissl, W. Ulrici, M. El-Metoui, A.-M. Vasson, A. Vasson, and A. Gavaix, “Neutral manganese acceptor in GaP: An electron-paramagnetic-resonance study,” *Phys Rev B* **54**, 10508–10515 (1996).

- ⁴⁹ A. Wolos, M. Palczewska, M. Zajac, J. Gosk, M. Kaminska, A. Twardowski, M. Bockowski, I. Grzegory, and S. Porowski, “Optical and magnetic properties of Mn in bulk GaN,” *Phys Rev B* **69**, 115210 (2004).
- ⁵⁰ J. Gosk, M. Zajac, A. Wolos, M. Kaminska, A. Twardowski, I. Grzegory, M. Bockowski, and S. Porowski, “Magnetic anisotropy of bulk GaN:Mn single crystals codoped with Mg acceptors,” *Phys Rev B* **71**, 94432 (2005).
- ⁵¹ W. Stefanowicz, D. Sztenkiel, B. Faina, A. Grois, M. Rovezzi, T. Devillers, F. d’Acapito, A. Navarro-Quezada, T. Li, R. Jakiela, M. Sawicki, T. Dietl, and A. Bonanni, “Structural and paramagnetic properties of dilute $\text{Ga}_{1-x}\text{Mn}_x\text{N}$,” *Phys Rev B* **81**, 235210 (2010).
- ⁵² I.L. Guy, S. Muensit, and E.M. Goldys, “Extensional piezoelectric coefficients of gallium nitride and aluminum nitride,” *Appl Phys Lett* **75**, 4133–4135 (1999).
- ⁵³ J. Blinowski, P. Kacman, and J.A. Majewski, “Ferromagnetic superexchange in Cr-based diluted magnetic semiconductors,” *Phys Rev B* **53**, 9524–9527 (1996).
- ⁵⁴ M. Sawicki, T. Devillers, S. Gałęski, C. Simserides, S. Dobkowska, B. Faina, A. Grois, A. Navarro-Quezada, K.N. Trohidou, J.A. Majewski, T. Dietl, and A. Bonanni, “Origin of low-temperature magnetic ordering in $\text{Ga}_{1-x}\text{Mn}_x\text{N}$,” *Phys Rev B* **85**, 205204 (2012).
- ⁵⁵ C. Śliwa, and T. Dietl, “Electron-hole contribution to the apparent s - d exchange interaction in III-V dilute magnetic semiconductors,” *Phys Rev B* **78**, 165205 (2008).
- ⁵⁶ A. Bonanni, T. Dietl, and H. Ohno, “Dilute Magnetic Materials,” in *Handbook of Magnetism and Magnetic Materials*, edited by J.M.D. Coey and S.S.P. Parkin, (Springer International Publishing, Cham, 2021), pp. 923–978.
- ⁵⁷ G. Kunert, S. Dobkowska, T. Li, H. Reuther, C. Kruse, S. Figge, R. Jakiela, A. Bonanni, J. Grenzer, W. Stefanowicz, J. von Borany, M. Sawicki, T. Dietl, and D. Hommel, “ $\text{Ga}_{1-x}\text{Mn}_x\text{N}$ epitaxial films with high magnetization,” *Appl Phys Lett* **101**, 022413 (2012).
- ⁵⁸ D. Sztenkiel, K. Gas, J.Z. Domagala, D. Hommel, and M. Sawicki, “Crystal field model simulations of magnetic response of pairs, triplets and quartets of Mn^{3+} ions in GaN,” *New J Phys* **22**, 123016 (2020).
- ⁵⁹ D. Sztenkiel, “Spin orbital reorientation transitions induced by magnetic field,” *J Magn Magn Mater* **572**, 170644 (2023).
- ⁶⁰ K. Gas, and M. Sawicki, “In situ compensation method for high-precision and high-sensitivity integral magnetometry,” *Meas Sci Technol* **30**, 085003 (2019).

Supplementary material

Spin Hall magnetoresistance in Pt/(Ga,Mn)N devices

J. Aaron Mendoza-Rodarte^{1,2*}, Katarzyna Gas^{3,4}, Manuel Herrera-Zaldívar², Detlef Hommel⁵, Maciej Sawicki^{3,6}, and Marcos H. D. Guimarães^{1*}

¹*Zernike Institute for Advanced Materials, University of Groningen, 9747 AG Groningen, The Netherlands*

²*Centro de Nanociencias y Nanotecnología-Universidad Nacional Autónoma de México, Ensenada, 22800-Baja California, México*

³*Institute of Physics, Polish Academy of Sciences, Aleja Lotnikow 32/46, PL-02668 Warsaw, Poland*

⁴*Center for Science and Innovation in Spintronics, Tohoku University, Katahira 2-1-1, Aoba-ku, Sendai 980-8577, Japan*

⁵*Lukasiewicz Research Network - PORT Polish Center for Technology Development, Stablowicka 147, Wrocław, Poland*

⁶*Research Institute of Electrical Communication, Tohoku University, Katahira 2-1-1, Aoba-ku, Sendai 980-8577, Japan*

Short-range superexchange mechanism in (Ga,Mn)N insulating systems

Mn-doped GaN systems are currently identified as diluted ferromagnetic semiconductors (DFS), and remain as one of the most prominent members of this family, despite the ferromagnetic coupling in (Ga,Mn)N is not mediated by itinerant carriers (holes). This stems from the fact that, importantly to this study, the Mn acceptor derived holes are so strongly localized (mostly due to p-d hybridization) on Mn acceptors¹ that in the absence of other doping or numerous charged point defects Mn-doped GaN remains insulating up to the highest (currently) available concentrations in epitaxy²⁻⁶. At these instances, Mn assumes a neutral acceptor oxidation state, Mn^{+3} (d^4 configuration) characterized by spin and orbital momentum quantum numbers $S = 2$ and $L = 2$, respectively⁷, and a strong single ion uniaxial magnetic anisotropy with respect to the wurtzite c -axis of GaN⁸⁻¹⁰. The latter proved to be controllable by an externally applied electrical field¹¹, via the inverse piezoelectric effect in GaN host lattice along the c axis¹².

As a consequence of the strongly insulating character of GaN enriched with Mn, the carrier-mediated coupling is precluded in (Ga,Mn)N. The observed low-temperature ferromagnetism is based on a short-range superexchange scenario^{2,13,14}, which, below the nearest-neighbor percolation threshold, earns its effectiveness from the ferromagnetic (FM) sign of the spin-spin exchange constants up to the nearest 30th neighbors^{14,15}, and the ferromagnetism is established in percolation fashion^{16,17}.

Details of the Pt/(Ga,Mn)N devices fabrication

Our devices were fabricated on a Ga_{1-x}Mn_xN (100 nm) single-phase epitaxial film. More details of the growth and characterization of the Ga_{1-x}Mn_xN films can be found in Ref.¹⁸. We patterned 25 μ m-wide, 200 μ m-long Hall bars using a 950K polymethyl methacrylate (PMMA) positive resist, with a solid content of 4% dissolved in ethyl lactate. To prevent charging effects during the electron beam exposure process, we spin-coated Electra-92 on top of the PMMA, which serves as a water-soluble conductive polymer. The device patterning was conducted using a Raith e-line 150 electron-beam lithography system with an acceleration voltage of 10 kV. For the development process, the Electra 92 layer is removed by immersing the sample in deionized water. Then, to develop the PMMA, the sample is immersed in a 1:3 mixture of isopropyl alcohol (IPA) and methylisobutylketon (MIBK). Next, a Pt (6 nm) layer is deposited using a sputtering machine with a base pressure better than 1×10^{-7} mbar, using an Ar plasma with a working pressure of 4×10^{-3} mbar with a power 50 W, resulting in a rate of 0.36 nm/s. Prior to deposition, the sample undergoes an Ar⁺ mild etching step with a power of 200 W to remove organic residues and a potential top oxide layer from the (Ga,Mn)N exposed surface, resulting in a clean and high-quality interface. A Ti (5 nm)/ Au (55 nm) thin layer was deposited to ensure electrical contact via an electron beam evaporation system. The lift-off process is carried out by immersing the sample in acetone at 45 °C, rinsing it with IPA, and blowing it dry with nitrogen gas. Finally, the devices are bonded to a 44-pin chip carrier.

The measurements are performed using a flow cryostat (Oxford Instruments) mounted between the poles of a room-temperature electromagnet with the magnetic field aligned to the in-plane direction with respect to the sample. The current is applied using a home-made current source, referenced by the output of a lock-in amplifier and the voltage is pre-amplified by a home-made

voltage pre-amplifier before being sent to the lock-in amplifier. We applied currents below 1 mA at low frequencies (<200 Hz) to avoid heating and high-frequency effects.

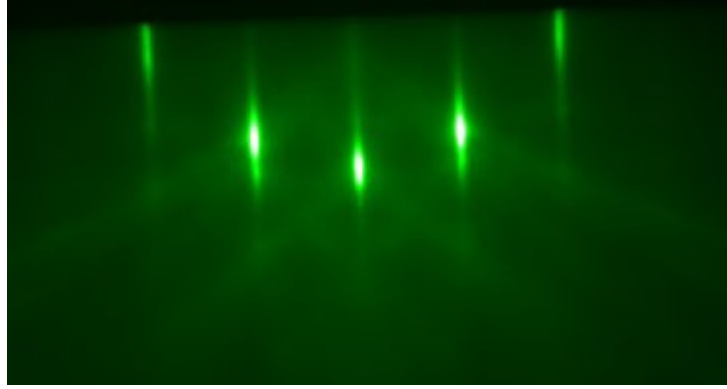


Figure S1. Reflection high-energy electron diffraction, RHEED, pattern along $[11\bar{2}0]$ azimuth observed after the growth and cooling the sample down below 200°C .

During the growth the surface quality of the layer has been investigated *in situ* by reflection high-energy electron diffraction (RHEED). The post growth $[11\bar{2}0]$ RHEED patterns collected after the growth (below 200°C) is shown in Fig. S1. The streaky and sharp RHEED pattern with clearly visible Kikuchi lines indicates that the (Ga,Mn)N surface is smooth and relatively free of oxides or other contaminants.

SQUID magnetometry measurements

The Curie temperature (T_{C}) of the magnetic layer used for the Pt/(Ga,Mn)N devices was previously assessed by five different methods by SQUID magnetometry, converging to the value of $T_{\text{C}} = 13.0 \pm 0.3$ K. More details can be found in Ref.¹⁸ where the magnetic layer for the devices shown in the main text is labelled as S605. The magnetization curves, M - H , for this sample are shown in Figure S2. We highlight the fact that the M - H curves presented in Figure S2 are representative of single-phase (Ga,Mn)N epitaxial layers^{18–20}. Importantly, we do not register any nonlinear magnetization at the weak field region above T_{C} , which confirms the single magnetic phase of the (Ga,Mn)N layer investigated here. Below $T_{\text{C}} \cong 13.0$ K M responses swiftly to the applied field already at very weak fields, yet it does not reach the complete saturation even at $\mu_0 H = 7$ T at $T = 2$ K. This behaviour highlights the fact that the M in (Ga,Mn)N is largely controlled by the single ion properties of the Mn^{3+} ions (described in the frame of the crystal field model) and

that the orbital contribution to M exhibits a much weaker dependence on H than the spin component does^{20,21}.

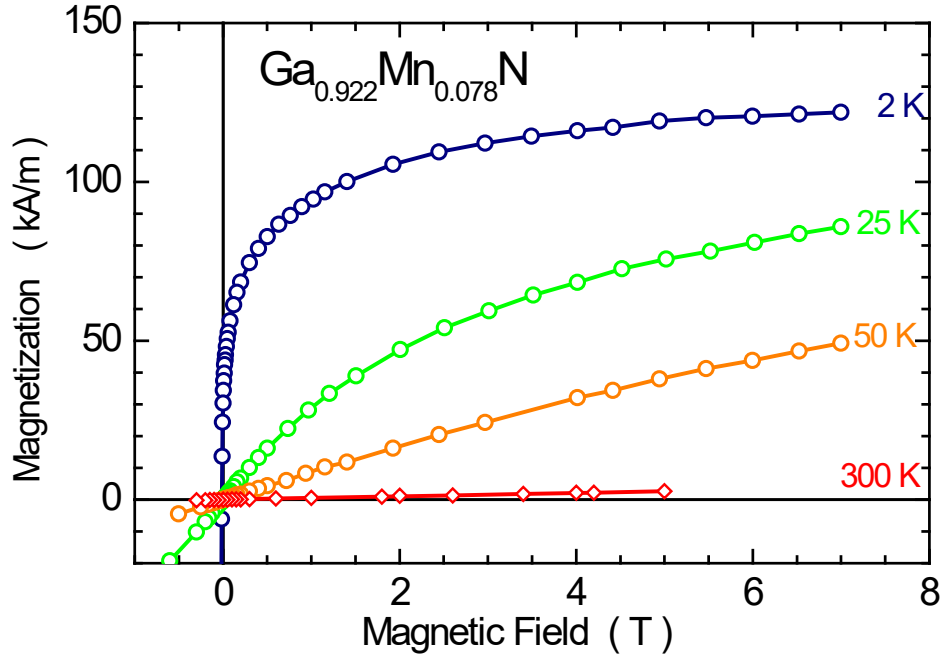


Figure S2. Magnetization, M , curves of the particular sample investigated in the main part of the letter at four selected temperatures. The magnetic field is applied in the plane of the sample (i.e. perpendicularly to the wurtzite c axis), which is the easy orientation for M in this material^{8–10}. The absolute value of M specific to the (Ga,Mn)N epilayer is established upon the technique allowing *in situ* compensation of the unwanted signal of the substrate (sapphire) described in Ref.²².

REFERENCES

- ¹ T. Dietl, F. Matsukura, and H. Ohno, “Ferromagnetism of magnetic semiconductors: Zhang-Rice limit,” *Phys Rev B* **66**, 33203 (2002).
- ² A. Bonanni, M. Sawicki, T. Devillers, W. Stefanowicz, B. Faina, T. Li, T.E. Winkler, D. Sztienkiel, A. Navarro-Quezada, M. Rovezzi, R. Jakiela, A. Grois, M. Wegscheider, W. Jantsch, J. Suffczyński, F. D’Acapito, A. Meingast, G. Kothleitner, and T. Dietl, “Experimental probing of exchange interactions between localized spins in the dilute magnetic insulator (Ga,Mn)N,” *Phys Rev B* **84**, 35206 (2011).

- ³ T. Yamamoto, H. Sazawa, N. Nishikawa, M. Kiuchi, T. Ide, M. Shimizu, T. Inoue, and M. Hata, “Reduction in Buffer Leakage Current with Mn-Doped GaN Buffer Layer Grown by Metal Organic Chemical Vapor Deposition,” *Jpn J Appl Phys* **52**, 08JN12 (2013).
- ⁴ R. Adhikari, W. Stefanowicz, B. Faina, G. Capuzzo, M. Sawicki, T. Dietl, and A. Bonanni, “Upper bound for the *s-d* exchange integral in *n*-(Ga,Mn)N:Si from magnetotransport studies”, *Phys Rev B* **91**, 205204 (2015).
- ⁵ L. Janicki, G. Kunert, M. Sawicki, E. Piskorska-Hommel, K. Gas, R. Jakiela, D. Hommel, and R. Kudrawiec, “Fermi level and bands offsets determination in insulating (Ga,Mn)N/GaN structures,” *Sci Rep* **7**, 41877 (2017).
- ⁶ K. Kalbarczyk, K. Dybko, K. Gas, D. Sztenkiel, M. Foltyn, M. Majewicz, P. Nowicki, E. Łusakowska, D. Hommel, and M. Sawicki, “Electrical characteristics of vertical-geometry Schottky junction to magnetic insulator (Ga,Mn)N heteroepitaxially grown on sapphire,” *J Alloys Compd* **804**, 415 (2019).
- ⁷ J. Kreissl, W. Ulrici, M. El-Metoui, A.-M. Vasson, A. Vasson, and A. Gavaix, “Neutral manganese acceptor in GaP: An electron-paramagnetic-resonance study,” *Phys Rev B* **54**, 10508 (1996).
- ⁸ A. Wolos, M. Palczewska, M. Zajac, J. Gosk, M. Kaminska, A. Twardowski, M. Bockowski, I. Grzegory, and S. Porowski, “Optical and magnetic properties of Mn in bulk GaN,” *Phys Rev B* **69**, 115210 (2004).
- ⁹ J. Gosk, M. Zajac, A. Wolos, M. Kaminska, A. Twardowski, I. Grzegory, M. Bockowski, and S. Porowski, “Magnetic anisotropy of bulk GaN:Mn single crystals codoped with Mg acceptors,” *Phys Rev B* **71**, 94432 (2005).
- ¹⁰ W. Stefanowicz, D. Sztenkiel, B. Faina, A. Grois, M. Rovezzi, T. Devillers, F. d’Acapito, A. Navarro-Quezada, T. Li, R. Jakiela, M. Sawicki, T. Dietl, and A. Bonanni, “Structural and paramagnetic properties of dilute $\text{Ga}_{1-x}\text{Mn}_x\text{N}$ ”, *Phys Rev B* **81**, 235210 (2010).
- ¹¹ D. Sztenkiel, M. Foltyn, G.P. Mazur, R. Adhikari, K. Kosiel, K. Gas, M. Zgirski, R. Kruszka, R. Jakiela, T. Li, A. Piotrowska, A. Bonanni, M. Sawicki, and T. Dietl, “Stretching magnetism with an electric field in a nitride semiconductor,” *Nat Commun* **7**, 13232 (2016).
- ¹² I.L. Guy, S. Muensit, and E.M. Goldys, “Extensional piezoelectric coefficients of gallium nitride and aluminum nitride,” *Appl Phys Lett* **75**, 4133 (1999).
- ¹³ J. Blinowski, P. Kacman, and J.A. Majewski, “Ferromagnetic superexchange in Cr-based diluted magnetic semiconductors,” *Phys Rev B* **53**, 9524 (1996).

- ¹⁴ M. Sawicki, T. Devillers, S. Gałęski, C. Simserides, S. Dobkowska, B. Faina, A. Grois, A. Navarro-Quezada, K.N. Trohidou, J.A. Majewski, T. Dietl, and A. Bonanni, “Origin of low-temperature magnetic ordering in $\text{Ga}_{1-x}\text{Mn}_x\text{N}$,” *Phys Rev B* **85**, 205204 (2012).
- ¹⁵ C. Śliwa, and T. Dietl, “Electron-hole contribution to the apparent s - d exchange interaction in III-V dilute magnetic semiconductors,” *Phys Rev B* **78**, 165205 (2008).
- ¹⁶ I.Ya. Korenblit, E.F. Shender, and B.I. Shklovsky, “Percolation approach to the phase transition in very dilute ferromagnetic alloys,” *Phys Lett A* **46**, 275–276 (1973).
- ¹⁷ A. Bonanni, T. Dietl, and H. Ohno, “Dilute Magnetic Materials,” in *Handbook of Magnetism and Magnetic Materials*, edited by J.M.D. Coey and S.S.P. Parkin, (Springer International Publishing, Cham, 2021), pp. 923–978.
- ¹⁸ K. Gas, J.Z. Domagala, R. Jakiela, G. Kunert, P. Dłuzewski, E. Piskorska-Hommel, W. Paszkowicz, D. Sztenkiel, M.J. Winiarski, D. Kowalska, R. Szukiewicz, T. Baraniecki, A. Miszczuk, D. Hommel, and M. Sawicki, “Impact of substrate temperature on magnetic properties of plasma-assisted molecular beam epitaxy grown $(\text{Ga,Mn})\text{N}$,” *J Alloys Compd* **747**, 946 (2018).
- ¹⁹ G. Kunert, S. Dobkowska, T. Li, H. Reuther, C. Kruse, S. Figge, R. Jakiela, A. Bonanni, J. Grenzer, W. Stefanowicz, J. von Borany, M. Sawicki, T. Dietl, and D. Hommel, “ $\text{Ga}_{1-x}\text{Mn}_x\text{N}$ epitaxial films with high magnetization,” *Appl Phys Lett* **101**, 022413 (2012).
- ²⁰ D. Sztenkiel, K. Gas, J.Z. Domagala, D. Hommel, and M. Sawicki, “Crystal field model simulations of magnetic response of pairs, triplets and quartets of Mn^{3+} ions in GaN ,” *New J Phys* **22**, 123016 (2020).
- ²¹ D. Sztenkiel, “Spin orbital reorientation transitions induced by magnetic field,” *J Magn Magn Mater* **572**, 170644 (2023).
- ²² K. Gas, and M. Sawicki, “In situ compensation method for high-precision and high-sensitivity integral magnetometry,” *Meas Sci Technol* **30**, 085003 (2019).